

# Impedance, Electrical and Dielectric behaviour of Tin Oxide Nanoparticle doped with Graphite, Graphene Oxide and Reduced Graphene Oxide

Benny Sebastian<sup>1,2,\*</sup>, C. George Thomas .<sup>2</sup> and B. Manoj.<sup>2</sup>

<sup>1</sup> Bharathiar University, Coimbatore, INDIA

<sup>2</sup> Department of Physics and Electronics, CHRIST University, Bengaluru, INDIA

\*E-mail: [benny.sebastian@christuniversity.in](mailto:benny.sebastian@christuniversity.in)

Received: 29 March 2021 / Accepted: 23 May 2021 / Published: 30 June 2021

Nanostructured materials have attained incredible interest in recent days due to their distinctive chemical, physical, mechanical, magnetic and optoelectronic properties. In the present study, metal nano particle ( $\text{SnO}_2$ ) was doped with graphite, graphene oxide (GO) and reduced graphene oxide (rGO) with various composition (1:100), (1:1) and (100:1) by weight ratio. The citrate-nitrate gel combustion method was used to prepare nanocrystalline  $\text{SnO}_2$  while GO and rGO were synthesized through modified Hummer's method. The preparation of  $\text{SnO}_2$ -rGO composites was done using a one-step hydrothermal process. The electrical and structural behaviour of the composites of graphite, GO and rGO mixed with  $\text{SnO}_2$  were elucidated by the impedance analyzer in the frequency range from 10Hz to 1MHz. It is observed that the composite of  $\text{SnO}_2$  with graphite and reduced graphene oxide have similar broad characteristics while  $\text{SnO}_2$  mixed with GO is exhibiting different properties which could be attributed to the presence of oxygen functionalities.

**Keywords:** Nanocomposites, Graphene oxide, Reduced graphene oxide, Tin oxide.

## 1. INTRODUCTION

Metal oxide nanostructures have attracted a lot of interest in recent days because of their distinctive chemical, physical, mechanical, magnetic and optoelectronic properties alongside its finite size and high surface to volume proportion. Tin oxide ( $\text{SnO}_2$ ) stands out as the most essential material because of its high level of transparency in the visible spectrum, physical and chemical association with adsorbed species, with a wide energy gap ( $E_g = 3.6$  eV) making it as a novel material [1-10].

Graphite is an allotrope of carbon having  $sp^2$  hybridization, excellent conductor of heat and electricity. Its properties can be altered by controlling the oxidation and reduction. The same carbon can have  $sp^3$  structure like diamond which is a bad conductor or it can be tuned to reduced graphene oxide

which is a semiconductor. Also, graphite can be changed to graphene oxide (GO) by modified Hummer's Method and upon reduction it turns to rGO. In terms of electrical conductivity, graphene oxide is often labelled as an electrical insulator, due to the disruption of its  $sp^2$  bonding networks. While reduced graphene oxide (rGO) acts like a semiconductor, the electrical conductivity of rGO can be regulated by varying the oxygen concentration. [11-17].

Tin oxide ( $SnO_2$ ) and its composite semiconductor have found wide applications in sensors, detectors and energy harvesting applications. Many researchers are interested in tin oxide-graphene composites due to possibility of enhancing properties like higher band gap, high surface area, chemical stability and electro catalytic activity. One can alter the resistance, capacitance, dielectric constants, tangent loss and AC conductivity of  $SnO_2$  nanoparticle by making composites with graphite, GO and reduced graphene oxide with variations in frequency. In the present study tin-oxide prepared by Gel combustion method is made composite with nanocarbon having conducting, semiconducting and insulating properties. These composites have variations in electrical properties. This can lead to various applications of such composites in lithium-ion batteries, super capacitors, biosensors and photo catalysis [18-24].

## 2. MATERIALS AND METHODS

### 2.1 Synthesis of nano-crystalline tin oxide

Tin oxide nanoparticles were prepared by gel combustion method followed by calcinations at high temperature as reported by our earlier study [1]. The synthesized  $SnO_2$  nanostructure was calcined at  $600^\circ C$  (873K) for two hours. The obtained product was used for making the composites and to investigate the various changes in the properties of nanocarbon- tin oxide composites.

### 2.2. Synthesis of tin oxide–nanocarbon composites

Modified Hummer's method was used to make graphene oxide from graphite powder and reduction of graphene oxide was further achieved by hydrothermal approach.

The nanocomposites of tin oxide –graphite, tin oxide-graphene oxide and tin oxide- reduced graphene oxide was made by mixing different ratios of respective compounds. Nanocomposites were prepared for various concentration ratios viz (100:1), (1:1) and (1:100), (by ratio of weight  $SnO_2$ : rGO) and designated as S1, S2, and S3 respectively [2-7]. Each sample was pressed into pellets by using hydraulic press. The pellets are further sintered at  $150^\circ C$  for 1 hour. To make proper electrical contact, the pellets were coated with silver paste on opposite sides. The diameter of the disc shaped pellets was about 13 mm. The electrical measurements were carried out by using a dielectric cell and impedance analyzer (Model: (LCR-8101G) with frequencies ranging from 10 Hz to 1MHz at room temperature with a voltage of 1V. For the electrical conductivity measurements, the capacitance, impedance ( $Z$ ), real and imaginary dielectric constants were measured over the same frequency range. The dependence of real

and imaginary dielectric constants, ac conductivity, dielectric loss, resistance and capacitance values as a function of frequency are calculated.

The impedance  $Z$  consists of real part and imaginary part. By expanding it on a complex plane, the individual parameters can be calculated. The impedance  $Z$  can be expressed as follows:

$$Z = \text{Real part (Re)} + \text{Imaginary part (Im)}. \quad (1)$$

$$\theta = \tan^{-1} (\text{Im}/\text{Re}) \quad (2)$$

$$Z' = |Z| \cos \theta \quad (3)$$

$$Z'' = |Z| \sin \theta \quad (4)$$

The value of real dielectric constant ( $\epsilon'$ ) is calculated by using the equation,

$$\epsilon' = (C_p d) / (\epsilon_0 A) \quad (5)$$

where  $\epsilon_0$  is the permittivity of free space ( $8.854 \times 10^{-12}$  F/m),  $d$  and  $A$  are the thickness and area of the respective sample pellet and  $C_p$  is the capacitance of the sample in Farad.

The resistivity,  $\rho = (R_s A) / d \quad (6)$

where  $R_s$  is the resistance of the pellet.

The conductivity,  $\sigma = 1/\rho \quad (7)$

The imaginary dielectric constant can be calculated by using the formula,

$$\epsilon'' = \epsilon' / (\omega C_p R) \quad (8)$$

where  $\omega$  is the angular frequency. The dielectric loss ( $\tan\delta$ ) can be calculated as the ratio of imaginary dielectric constant to real dielectric constant.

$$\tan\delta = \epsilon'' / \epsilon' \quad (9) [5]$$

### 3. RESULTS AND DISCUSSION

#### 3.1 Electrical analysis of Graphite –SnO<sub>2</sub> composite

The dependence of electrical behavior of graphite-SnO<sub>2</sub> composite is studied in the frequency range (10Hz – 1MHz) and are presented in the following session.

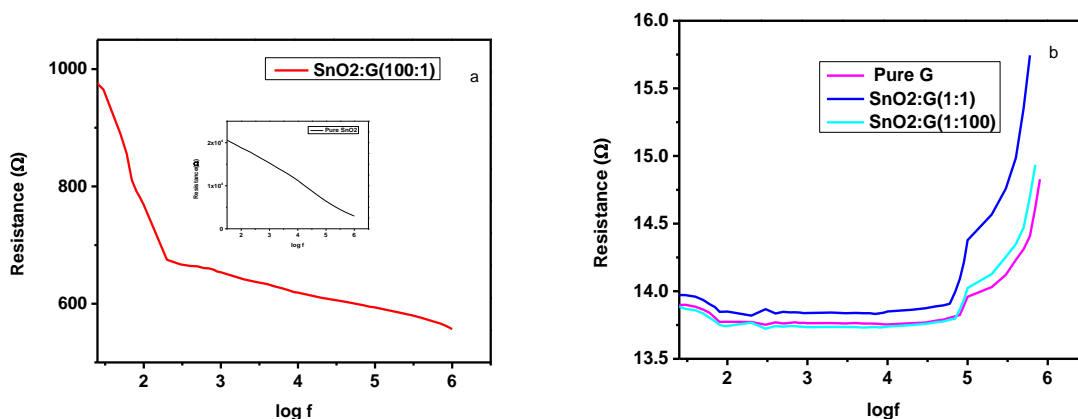


**Figure 1.** Variation of the resistance as function of frequency for SnO<sub>2</sub>- G (Graphite) composites

The ac resistance of the pure Graphite(G) and tin oxide - Graphite composites are presented in Figure 1. and that of pure SnO<sub>2</sub> is depicted in Figure 1(inset). The resistance clearly follows the trend of variation in conductivity with frequency indicating a transition, from a semiconductor to a conductor. The value of resistance of pure SnO<sub>2</sub> is found to be  $20 \times 10^3 \Omega$  and is linearly decreasing with increase in frequency. At 1MHz it is found to be 2.717 k $\Omega$  exhibiting a decrease of 8-fold. Upon adding graphite to SnO<sub>2</sub> in the ratio 100:1 by weight, the resistance at low frequency is found to be 1k $\Omega$  and the value is drastically lowered to 0.55 k $\Omega$  at 1MHz. On the other hand, when the composition of SnO<sub>2</sub>: Graphite is changed to (1:1) and (1:100) ratio, the resistance of the composite is altered altogether and is in the range of pure graphite as depicted in Fig 1(b). It is also worthwhile to mention that at low frequencies, the resistance is more or less constant (100 Hz to 100 kHz), above which there is a variation in resistance marginally. It is inferred that the composite has different AC resistance at various frequencies. It is also depending upon the amount of SnO<sub>2</sub> in graphite composite. So, by altering the proportion of both materials, one can easily tailor the electrical resistance of the composite [25-29].

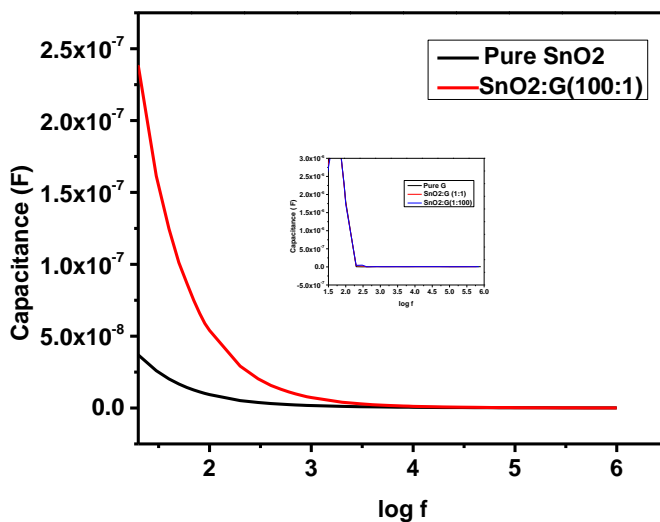


**Figure 2.** Variation of capacitance as function of frequency for SnO<sub>2</sub>- Graphite composites

The capacitance behavior of the SnO<sub>2</sub>-Graphite composite in terms of frequency versus capacitance is presented in Figure 2. SnO<sub>2</sub> nanostructure shows a capacitance of  $3.71 \times 10^{-8}$  F at low frequency and is lowered to  $6.62 \times 10^{-10}$  F at high frequency. There is not much variation in the capacitance value for a wide range (1kHz – 1MHz). But the (100:1) composite exhibit a capacitance value of  $2.30 \times 10^{-7}$  F at low frequency which shows a sixfold increase. (The capacitance values of other composites are as shown in inset) The capacitance value is exponentially decreased with increase in frequencies and constant at high frequency exhibiting the same trend as that of pure SnO<sub>2</sub>. For the composites, the value of capacitance is noted as  $3.6 \times 10^{-6}$  F, which is 100 times more than that of pure SnO<sub>2</sub>. This value is drastically reduced to  $5.68 \times 10^{-8}$  F at high frequency [30-36].

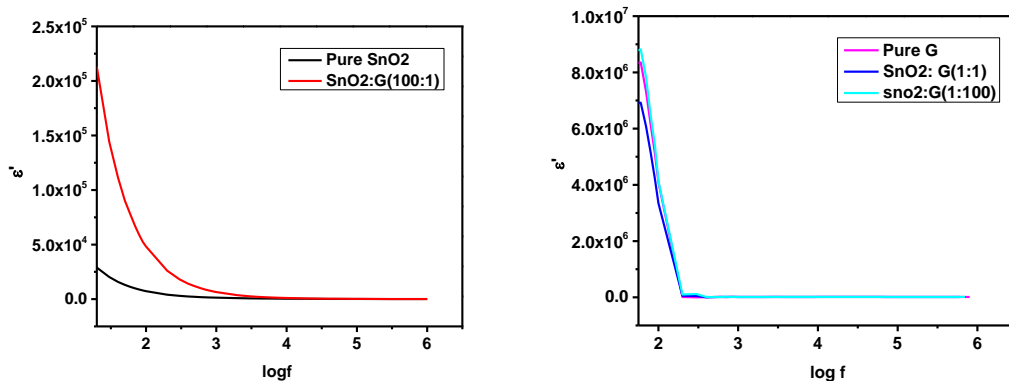


**Figure 3.** Variation of real dielectric constant as function of frequency for SnO<sub>2</sub>- Graphite composites

The dielectric strength of the composite is estimated using the expressions equations (5) and (8) The real part of the dielectric strength of the composite materials are depicted in Figure 3 The real value of the dielectric strength ( $\epsilon'$ ) of SnO<sub>2</sub> is found to be  $2.92 \times 10^4$  at 20 Hz and exponentially decays at higher frequencies. The composite 100: 1 shows the dielectric strength be  $2.12 \times 10^5$  at the same frequency. The other composites like (1:1), (1:100) & Graphite (G) shows higher dielectric strength at low frequency which decreases with increase in frequency. This could be as a result of charge carriers accumulating at grain boundary and is in agreement with the reported study [5-9, 37].

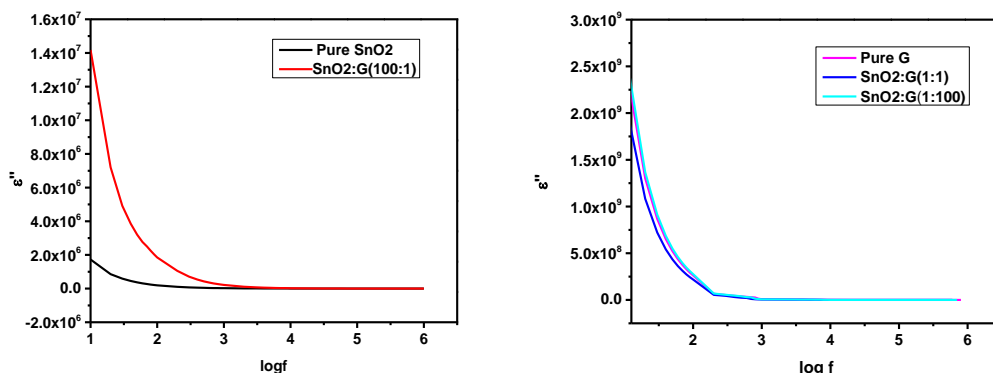


**Figure 4.** Variation of imaginary dielectric constant as a function of frequency for SnO<sub>2</sub>-Graphite composites

The imaginary part of the dielectric strength ( $\epsilon''$ ) also exhibiting the same behavior as shown in Figure 4. At low frequency it shows dependence on frequency and drastically decreases as the frequency increases at room temperature. From the graphs (Figures 3 & 4), it is evident that both real and imaginary parts of the complex dielectric permittivity are frequency dependent.

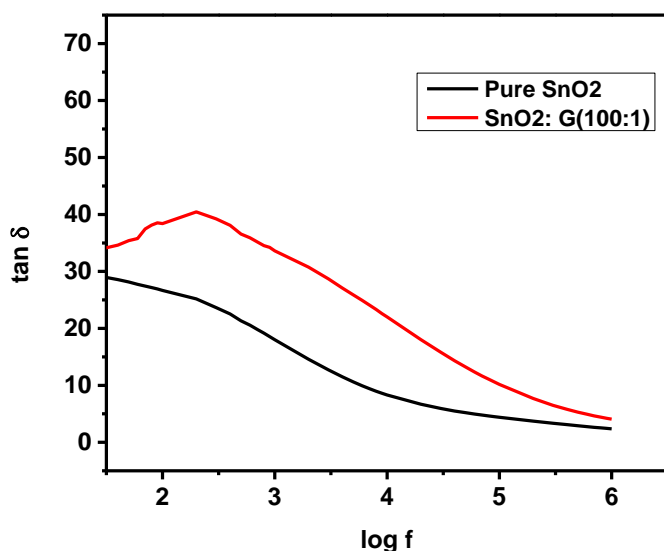


**Figure 5.** Variation of dielectric loss ( $\tan \delta$ ) as function of frequency for SnO<sub>2</sub>- Graphite composites

It is a known fact that the dielectric loss represents the loss of energy in the system. The variation in loss of the dielectric strength ( $\tan \delta$ ) is exhibiting an interesting trend for pure SnO<sub>2</sub> and composite (100:1) ratio as presented in Figure 5. The variation in dielectric loss of the SnO<sub>2</sub> is quicker than that of the composite with increase in frequency.

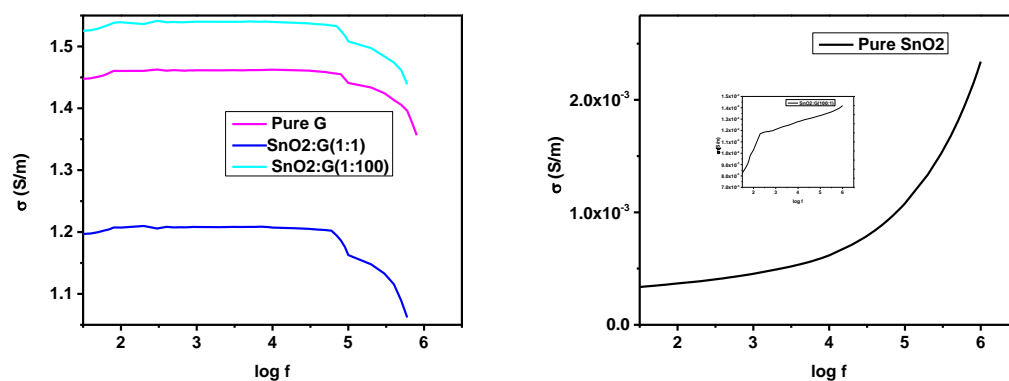


**Figure 6.** Variation of ac conductivity as function of frequency for SnO<sub>2</sub>-Graphite composites.

The AC conductivity of the obtained composite is compared with that of SnO<sub>2</sub> and graphite as depicted in Figure 6. It is clearly observed that the conductivity is independent of frequency indicating a dc trend in the case of pure graphite, graphite- SnO<sub>2</sub> composite with the ratios (1:1) and (1:100). The pure SnO<sub>2</sub> shows conductivity of  $3.267 \times 10^{-4}$  S/m at low frequency and exponentially increases to  $2.32 \times 10^{-3}$  S/m at 1 MHz. This is attributed to the fact that ac conductivity is due to high polarization of charge carriers and ac-hopping conduction of the localized sites [8]. But the composite (100:1) is

showing a linear increase till 137 Hz and thereafter shows a systematic variation. The composite 1:1 exhibit a conductivity at 1.2 S/m. Graphite being a good conductor showed 1.45 S/m till 79.43 kHz. The frequency independent behavior of conductivity of graphite is depicted in the graph. The conductivity of composite (1:100) is higher (1.54) than the other two composites.

It is noticed that upon addition of graphite to SnO<sub>2</sub> nanostructure the electrical behavior of the composite is modified. Capacitance and dielectric behaviors of the composite has shown variations with increase in frequency.

### 3.2 Electrical analysis of SnO<sub>2</sub> – GO composite

The electrical behavior of SnO<sub>2</sub> composite with Graphene Oxide is investigated and presented in the following section.

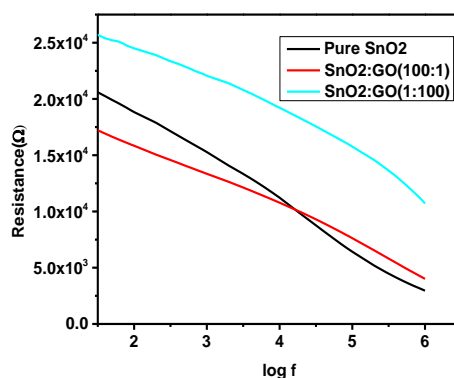


**Figure 7.** Variation of resistance as function of frequency for SnO<sub>2</sub>- GO composites

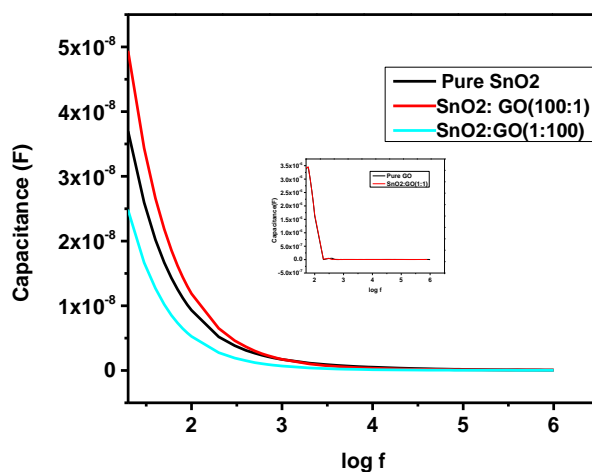


**Figure 8.** Variation of capacitance as function of frequency for SnO<sub>2</sub>- GO composites

The variation of resistance of the composites of SnO<sub>2</sub> and GO of the concentrations (100:1), (1:1) and (1:100) are studied along with pure SnO<sub>2</sub> and presented in Figure 7. In the (100:1) and (1:100)

composite of GO and SnO<sub>2</sub>, the resistance shows the same trend as that of SnO<sub>2</sub> exhibiting high resistance at low frequencies. Again, at 16.2 kHz, the resistance of (100:1) composite is becoming more than that of SnO<sub>2</sub>.

The capacitance behavior of the SnO<sub>2</sub>-GO is depicted in Figure 8. The SnO<sub>2</sub>-GO composite (100:1) exhibit a capacitance of  $4.88 \times 10^{-8}$  F while for (1:100) composite, the capacitance value halved ( $2.48 \times 10^{-8}$  F). But in the same weight proportion of SnO<sub>2</sub>-Graphite composite, the capacitance is about  $2.37 \times 10^{-7}$  F. There is reduction of capacitance value by ten-fold. While the capacitance of GO and 1:1 composite has the capacitance value of  $3.44 \times 10^{-6}$  F. This is an appreciable value compared to the value of SnO<sub>2</sub>-Graphite composite. This indicates that adding the GO to the SnO<sub>2</sub> matrix in the ratio (1:1) has enhanced the capacitance of the composite

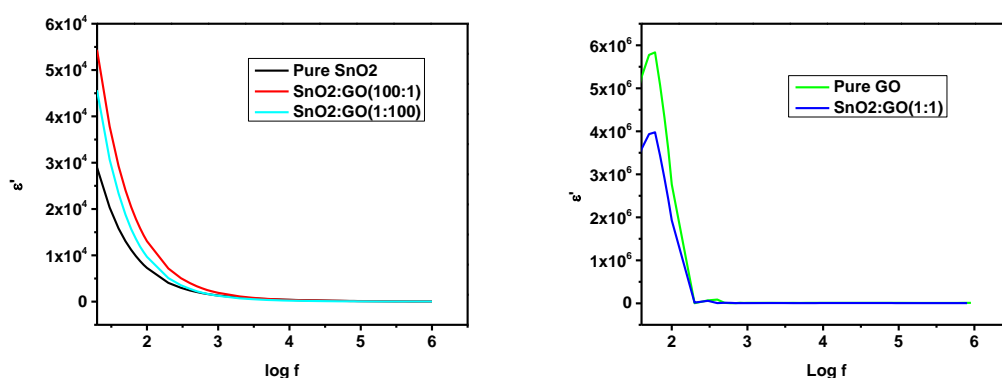


**Figure 9.** Variation of real dielectric constant as function of frequency for SnO<sub>2</sub>- GO composites

The real part of dielectric strength of SnO<sub>2</sub>-GO composite is presented in Figure 9. The dielectric constant decreases with increase in frequency. This behavior is a general trend for any dielectric material which can be attributed to the scattering of charge carriers at high frequencies and also the fast variation of electric field as a result of the frequency variation. The decrease of ( $\epsilon'$ ) with frequency can be attributed to the fact that at low frequencies ( $\epsilon'$ ) for polar materials is given by the sum of all the polarizability components which include ionic, electronic, orientation and interface [8]. It is reported that the space charge polarization which occurs due to impedance mobile charge carries by interfaces and usually takes place at  $1$  to  $10^3$  Hz. All these contribute to the total polarization of the dielectric material. The orientation polarization decreases as the frequency is increased because it takes longer than electronic and ionic polarization. The dielectric constant decreases as a result, reaching a constant value at higher frequencies, leading to interfacial polarization [6]. The dielectric values of pure GO and the composite of GO and tin oxide (1:1) are depicted in Figure 9 (b) which shows the values  $5.79 \times 10^4$  F/m and  $3.94 \times 10^4$  F/m respectively at low frequencies. But at 212.8 kHz, its value is lowered to  $1.434 \times 10^4$ . But in the case of the composites (100:1), and (1:100) they exhibit the same trend as that of pure SnO<sub>2</sub>.



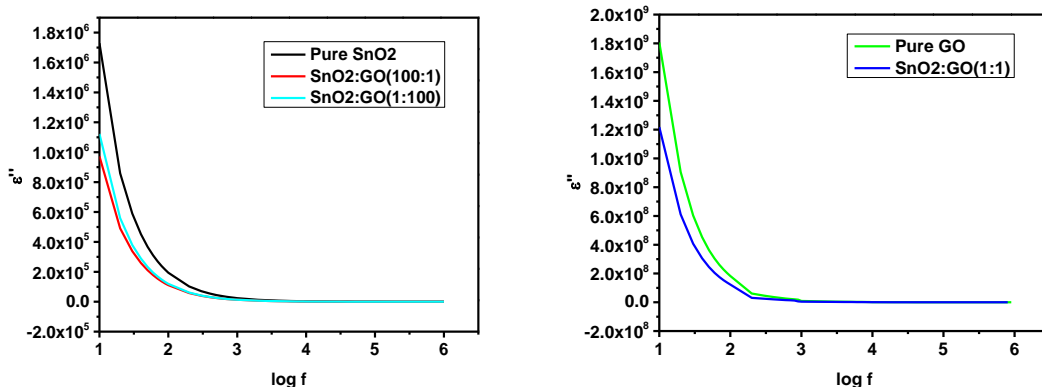


**Figure 10.** Variation of imaginary dielectric constant as function of frequency for SnO<sub>2</sub>- GO composites.

The imaginary part of the dielectric strength is also showing the same trend as shown in Figure 10(a) which is similar like that of the real part as depicted in Figure 9(a). It is obvious that ( $\epsilon''$ ) decreases as frequency increases. The decrease in the imaginary part of the dielectric constant with frequency can be explained by the fact that migration ions are the key cause of decrease in the imaginary part of the dielectric constant at lower frequencies. Because of the contribution of ion hop and conduction loss of ion migration in addition to ion polarization, the imaginary part of the dielectric constant at low and moderate frequencies has high values [6]. The ion vibration may be the only source of the imaginary component of the dielectric constant at high frequencies, so ( $\epsilon''$ ) decreases as frequency increases.

The real and imaginary dielectric constants have shown a 10-fold increment with SnO<sub>2</sub>-GO composite.

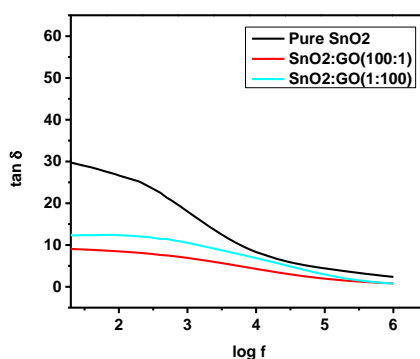


**Figure 11.** Variation of dielectric loss ( $\tan \delta$ ) as function of frequency for SnO<sub>2</sub>-GO composites

Figure 11. shows the variation of tangent loss as a function of frequency. The tangent loss shows very much low value for the composite compared to that of pure SnO<sub>2</sub> showing that these composites are well-suited to electronic applications such as capacitor fabrication [6]. While that of (1:100) and (100:1)

composite shows a decrease in trends with increase in frequency (For SnO<sub>2</sub>, it is 29.76 to 2.43, for (1:100) composite, it is 12.47 to 1.022 and for (100:1) composite, it is 8.95 to 1.022).

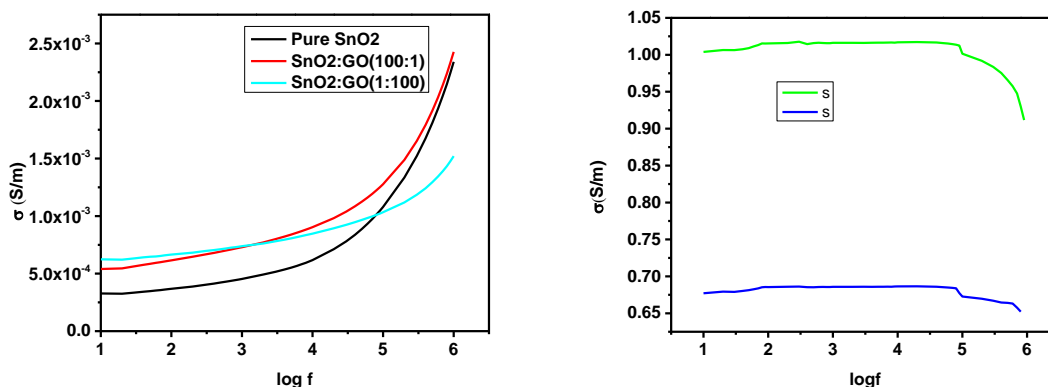


**Figure 12.** AC conductivity as function of frequency for SnO<sub>2</sub>-GO composites

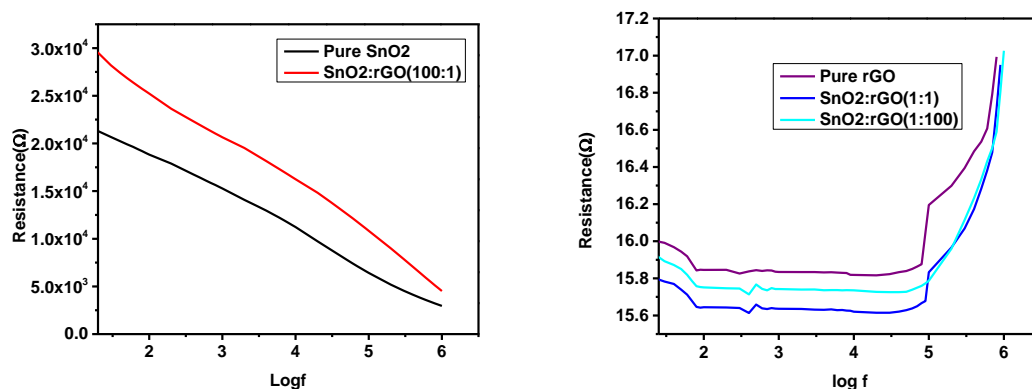
The AC conductivity of the tin oxide- graphene oxide composite is depicted in the figure 12. The interface charge polarization and intrinsic electric dipole polarization are thought to be responsible for the frequency dependence of ac conductivity. The pumping force of the field, which enables the transfer of charge carriers between different localized states as well as the liberation of trapped charges from different trapping centres, may explain the increase in ac conductivity with an applied field frequency. There is more charge accumulation at the electrode interface in the low frequency field, resulting in a decrease in the number of mobile ions. As a result, charge carrier mobility and number are limited, resulting in low conductivity. Frequency independence behavior of conductivity in low frequency region is also observed [6]. The ac conductivity of pure GO and the composite (1:1) have shown a decrease (0.679) compared to SnO<sub>2</sub>-Graphene oxide composite. When the tin oxide-GO composite ratios (100:1) and (1:100) are analyzed, they show a similar trend as that of SnO<sub>2</sub>. Also, on comparing the SnO<sub>2</sub>-GO composite with that of SnO<sub>2</sub>-Graphite composite, one can observe the (1:100) composite in both cases showing drastic variation in all the properties.

Pure SnO<sub>2</sub> and the composites (100:1) and (1: 100) of GO form a group which shows similar trends of change of properties unlike the graphite composites where (100:1) and pure SnO<sub>2</sub> exhibit same set of behaviors.

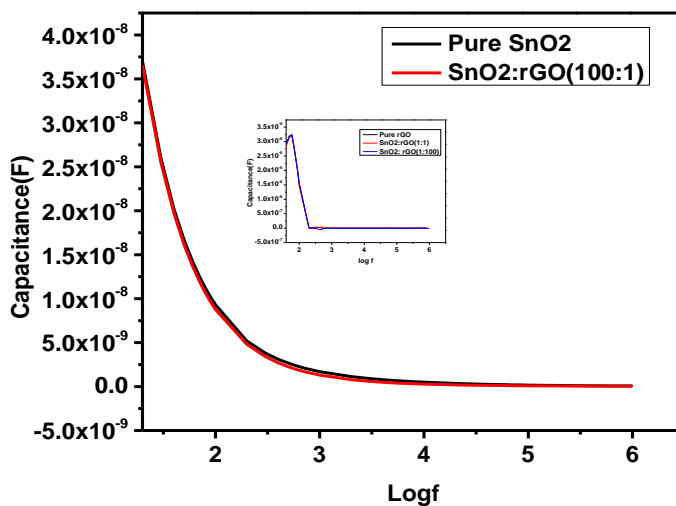
### 3.3. Electrical analysis of oxide Tin oxide- Reduced Graphene composite

Figure 13 depicts the ac resistance of the SnO<sub>2</sub>: rGO composites. The behaviour of rGO and the composite of SnO<sub>2</sub>-rGO in the ratio (1:1) exhibit similar as that of GO- SnO<sub>2</sub> (1:1) composite. The resistance values are almost same. The resistance of (100:1) composite is varying from 29.39 kΩ to 4.58 kΩ. The resistance of the (1:100) composite (SnO<sub>2</sub>: rGO) is very low similar to the value of pure rGO.

When one has more presence of SnO<sub>2</sub> as in the case of the composite (100:1) and (1:1), the SnO<sub>2</sub> characteristics prevails.



**Figure 13.** The variation of resistance as function of frequency for SnO<sub>2</sub>-rGO composites



**Figure 14.** The variation of capacitance as function of frequency for SnO<sub>2</sub>- rGO composites

The capacitance behavior of SnO<sub>2</sub>: rGO composite is depicted in Figure 14. Here it is seen that pure SnO<sub>2</sub> and SnO<sub>2</sub>: rGO in the ratio (100:1) have similar capacitance behavior. It is to be noted that the behaviour rGO is similar to that of graphene oxide.

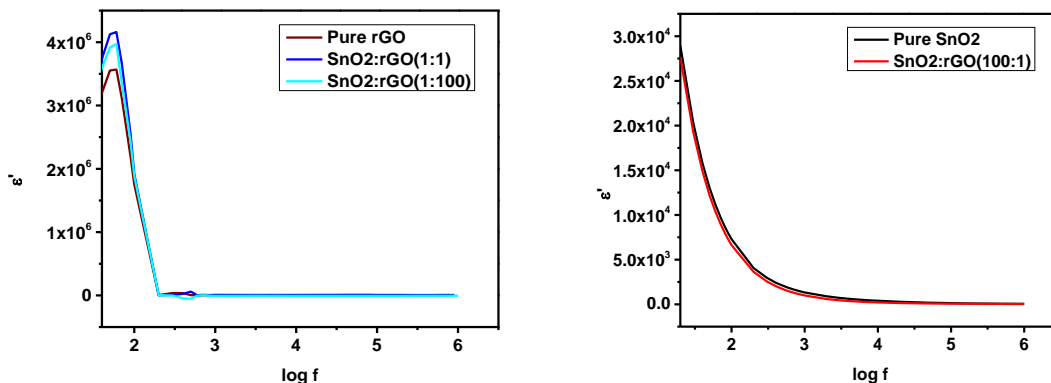


**Figure 15.** Variation of real dielectric constant as function of frequency for SnO<sub>2</sub>- rGO composites

Figure 15. shows the variation of real dielectric constant as function of frequency for SnO<sub>2</sub>- rGO composites. The dielectric constant decreases with increasing frequency and becomes fairly steady at high frequencies, as seen in the graph. This behavior can be explained in terms of Maxwell-Wagner-Sillars effect [34]. Charge carriers can easily migrate and accumulate at grain boundaries as a result of this operation, contributing to a high dielectric constant value at low frequencies. Due to inhomogeneous dielectric structure, the higher value of can also be explained in terms of space charge polarization. With higher frequencies, the polarization decreases until it reaches a nearly constant value.

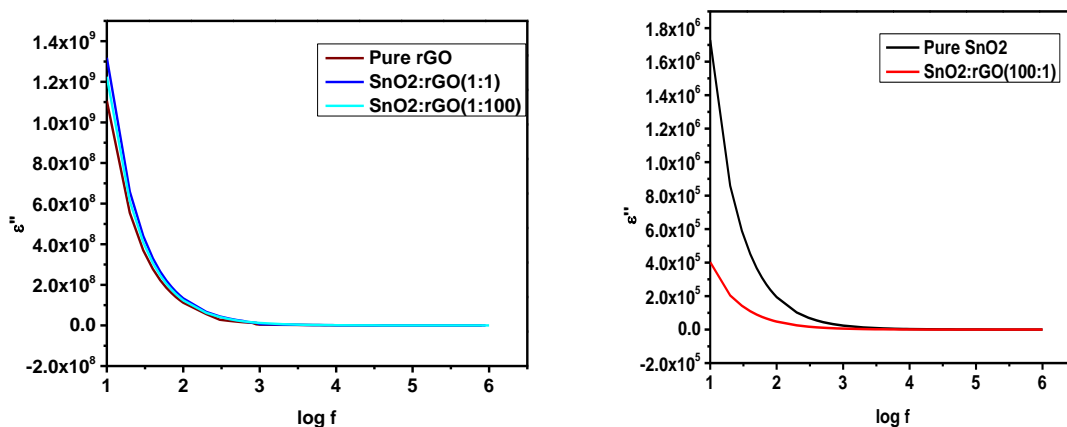


**Figure 16.** Variation of imaginary dielectric constant as function of frequency for SnO<sub>2</sub>-r GO composites.

Figure16. depicts the response of the imaginary dielectric constant for the SnO<sub>2</sub>- rGO composite with frequency. At lower frequencies, both the real ( $\epsilon'$ ) and imaginary ( $\epsilon''$ ) parts of the dielectric undergo a sharp decrease before being nearly constant at higher frequencies. This drop in dielectric constant with increasing frequency may be due to dielectric relaxation, a phenomenon that indicates that charge carrier localization is not stable and that frequency disturbances influence the charge carrier. The higher

dielectric constant value can also be explained by the interfacial/space charge polarization caused by a non-homogeneous dielectric structure, such as porosity and grain structure in nanocomposite [35]. The presence of tin oxide in the composite determines the dielectric behavior of the material. So, when the tin oxide – reduced graphene ratio is in (100:1), the behavior is that of tin oxide. Similar characteristics was reflected in the case of reduced graphene oxide and its composites.

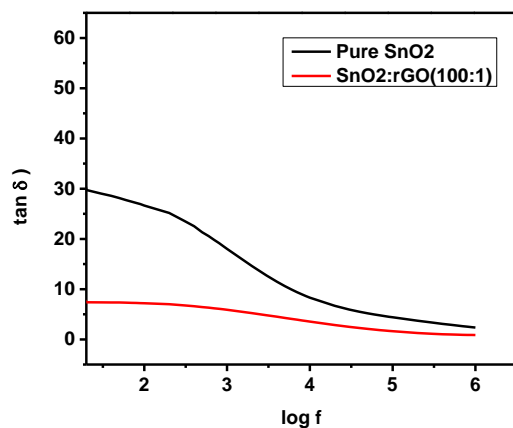


**Figure 17.** Variation of dielectric loss ( $\tan \delta$ ) as function of frequency for SnO<sub>2</sub>-rGO composites

The tangent loss is depicted in Figure 17. It is observed from Figure 17 that a comparatively high dielectric loss at low frequency with to pure tin oxide than in ratios of rGO- SnO<sub>2</sub>nanocomposite (100:1). This may be attributed to the high resistivity at low frequencies. Also, the tangent loss shows very much low value for the composite compared to that of pure SnO<sub>2</sub>.

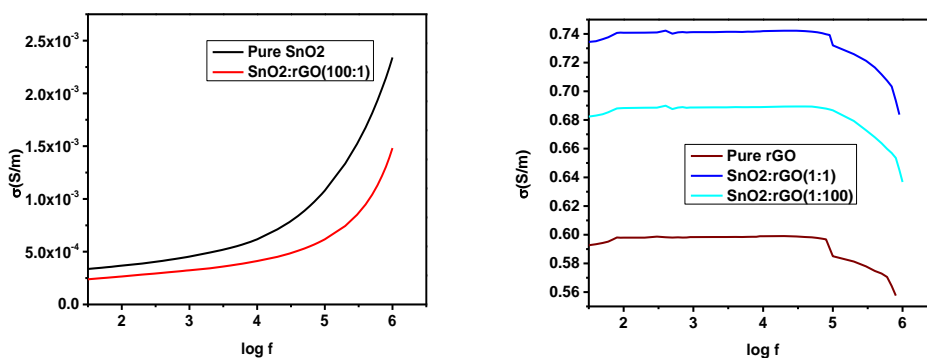


**Figure 18.** Variation of AC conductivity as function of frequency for SnO<sub>2</sub>-rGO composites

The AC conductivity response of SnO<sub>2</sub>-rGO composites is depicted in the Figures 18. When the composite is in the ratio (100:1), the conductivity increases linearly with change in frequency on a logarithmic scale. This also shows the ion transportation process in an ac electric field over a broad time scale. At the Wagner–Maxwell–Sillars region, the real conductivity values are found to be inversely

proportional to frequency. It is clear from the figures that the dominance of rGO and thereby the behavior of the composite in the ratio (1:100) & (1:1) is similar to rGO.

The behavioral electric properties of graphite and reduced graphene oxide are matching with the composites of SnO<sub>2</sub> -graphite and SnO<sub>2</sub>-rGO in the ratio 100:1. Both graphite and rGO, when doped with SnO<sub>2</sub> show high value of dielectric strength which means the conductivity is less.

#### 4. CONCLUSIONS

The present study compares the electrical behavior of various composition of SnO<sub>2</sub> with the carbon composites. Tin oxide was formed composite with graphite, graphene oxide and reduced graphene oxide with varying contents (1:100), (1:1) and (100:1) was successfully synthesized. It is observed that the composite of SnO<sub>2</sub>: graphite and SnO<sub>2</sub>: reduced graphene oxide has similar broad characteristics. SnO<sub>2</sub>: GO composite is exhibiting different properties which may be attributed to the presence of oxygen functionalities. It is worthwhile to mention that (100:1) composite of SnO<sub>2</sub>: GO composite is showing high value of resistance compared to other compositions. It is seen that in all composites, the real and imaginary part of the dielectric strengths have maximum value at low frequencies below 1 kHz which is mainly as a result of charges accumulated at the grain boundary. The dielectric constant decreases as the frequency changes since the space charge polarization gradually decreases, allowing the electronic and atomic contributions to take over. This can also be explained through the Wagner-Maxwell-Sillars effect. This occurs due to the contribution of charge accumulation by electrode interface. This also may be due to the alignment of dipoles with the direction of the applied field. The dielectric strength decreases as the frequency rises, possibly due to charge carrier scattering and the rapid deviation of the electric field.

#### AUTHOR CONTRIBUTIONS:

B.S contributed to the experimental design, procedure and carried out the experimental characterization and analysis. G.T.C supervised the work and extended periodic discussions. B.M contributed to the analysis of the data, correction of the whole manuscript.

#### CONFLICT OF INTEREST.

There is no conflict of interest among the authors of the manuscript.

#### DECLARATION:

The authors hereby declare that the manuscript is a record of original and independent research work done.

#### References

1. Benny Sebastian, C. George Thomas and B. Manoj, *Asian Journal of Chemistry*, 29 (2017)875.
2. Dutta Dipa, Chandra Sudeshna, K Swain Akshaya and Bahadur Dharendra, *Analytical Chemistry ACS Publications*, 86 (2014)5914.
3. Hazra Surajit Kumar and Basu Sukumar, *Journal of Carbon Research*, 2 (2016)12.

4. Lingfeng Jin, Weigen Chen, He Zhang, Gongwei Xiao and Chutian Yu, *Applied Science*, 7 (2017)17.
5. Ameer Azam, Arham S. Ahmed, M. Chaman, and A.H. Naqvi, *Journal of Applied physics*, 108 (2010)094329.
6. Virginia Mututu, A.K.Sunita, Riya Thomas, Mayank Pandey and B. Manoj, *Int. J. Electrochem. Sci.*, 14 (2019)3752.
7. AN. Mohan. B. Manoj and S. Panicker, *Scientific Reports*, 9(2019)1
8. Riya Thomas, E. Jayaseeli, N.M. Sushmita Sharma and B. Manoj, *Results in Physics*, 10 (2018)633.
9. Benny Sebastian, C. George Thomas and B. Manoj, *Research Journal of Chemistry and Environment*, 24(2020)23.
10. T.Riya and B. Manoj, *Materials today: Proceedings, Science Direct, Elsevier*, 43(6)(2021), 3424
11. B. Manoj, *Asian Journal of Chemistry*, 26(2014)4553.
12. W.B. Soltan, S. Nasri, M.S. Lassoued and S. Ammar, *Journal of Materials Science: Materials in Electronics*, 28 (2017)6649.
13. Rahmouni, M. Smari, B. Cherif, E. Dhahriband and K. Khirouni, *Dalton Transactions*, 44 (2015)10457.
14. B. Manoj, *Journal of environmental research and development* 6 (3A)(2012)654.
15. B. Manoj, *Research Journal of Biotechnology*, 8(3)(2013)49.
16. Madhadidevi and Ashokkumar, *Journal of Applied Polymer*, 137(2017)455883.
17. Lanje S. Jsharma, R.B. Pode and R.S. Ningthoujam, *Archives of Applied science research*, 2(2010)127.
18. M. Devi and Kumar, *A Journal of Applied Polymer*, 45883 (2017)1.
19. Shing Chung Wong, Erwin M Wouterson and EricM Sutherland, *Journal of Vinyl & Additive technology*, 12(2006)127.
20. D. Wang, X. Zhang, J.W. Zha, J. Zhao, Z.M. Dang and G.H.Hu, *Polymer*, 54(2013)1916.
21. B. Srinivasa Rao, B. Rajeshkumar, V. Rajagopal Reddy, T. Subba Rao and G. Venkata chalapathi, *Chalcogenide Letters*, 9(2012)517.
22. O.J. Dada and Villaroman, *Journal of Electrochemical society*, 166(2019) D21.
23. Md. Aatur Rehman and Gwiy-Sang Chung, *Journal of alloys and compounds*, 581(2013)724.
24. N. Manjula, G. Selvan, R. Perumalsamy, R. Thirumamagal, A. Ayeshamariam, and M. Jayachandran, *Int. J. Nanoelectronics and Materials*, 9(2016)143.
25. T. Prodromakis and C. Papavassiliou, *Applied Surface Science*, 255(2009)6889.
26. Nitesh Shukla and D.K. Dwivedi, *Journal of Asian ceramics and Societies*, 4(2016)178.
27. Chia-Chin Chang, Li-Chia Chen, Tai-Ying Hung Yuh-Fan Su, Huang-Kai Su, Jarrn-Horng Lin, Chih-Wei Hu, Lakshmanan Saravanan and Tsan-Yao Chen, *Int. J. Electrochem. Sci.*, 13(2018)11762.
28. R Thomas, E Jayaseeli, N.M.S. Sharma and B. Manoj. *Results in Physics*, 10(2018)633.
29. A.V. Ramya, A.N. Mohan and B. Manoj, *Materials Science-Poland*, 34 (2)(2016)330.
30. Adrian Rado, Patryk Włodarczyk and Dariusz Łukowiec, *Physica E: Low-dimensional Systems and Nanostructures*, 99(2018)82.
31. A. Ahmed, M.N. Siddique, T. Ali and P. Tripathi, *Advanced power technology*, 29(2018)3415.
32. Juman A. Nazer, Zainab W. Ahmed and Wadad J. Fendi, *Egyptian Journal of Chemistry*, 64 (2021)487.
33. Ayeshamariam, C.Sanjeeviraja, and R. Perumal Samy, *Journal on Photonics and Spintronics*, 2(2) (2013)2324.
34. M. Pandey, M. Balachandran, G.M. Joshi, N.N. Ghosh and A.S. Vendan, *Journal of Materials Science: Materials in Electronics*, 30(3)(2018)2136.
35. Farheen and Azra Praveen, *AIP Proceedings*, 2220(1) (2020)020196.
36. Anoushka K. Das, Joselyn E. Abraham, Mayank Pandey and B. Manoj, *Materials Today: Proceedings*, 24(2020)2108.

37. M.V. Chittan, C.M. Kumar and B.R. Kumar, *AIP Conference Proceedings*, 1992(1)(2018)040009.

© 2021 The Authors. Published by ESG ([www.electrochemsci.org](http://www.electrochemsci.org)). This article is an open access article distributed under the terms and conditions of the Creative Commons Attribution license (<http://creativecommons.org/licenses/by/4.0/>).